ACS Partner Journal

CHEM & BIO ENGINEERING

pubs.acs.org/ChemBioEng

Article

Non-monotonic Information and Shape Evolution of Polymers Enabled by Spatially Programmed Crystallization and Melting

Xing Zhang, Yichen Zhou, Mengzhe Han, Ying Zheng, Junfeng Liu, Yongzhong Bao, Guorong Shan, Chengtao Yu,* and Pengju Pan*

Cite This: *Chem Bio Eng.* 2024, 1, 790−797

Read Online

ACCESS | Metrics & More | Article Recommendations | Supporting Information

ABSTRACT: Stimuli-responsive polymer materials are a kind of intelligent material which can sense and respond to external stimuli. However, most current stimuli-responsive polymers only exhibit a monotonic response to a single constant stimulus but cannot achieve dynamic evolution. Herein, we report a method to achieve a non-monotonic response under a single stimulus by regionalizing the crystallization and melting kinetics in semicrystalline polymers. Based on the influence of cross-linking on the crystallization and melting kinetics of polymers, we employ light to spatially regulate the cross-linking degree in polymers. The prepared material can realize the self-evolved encryption of pattern information and the non-monotonic shape evolution without complex multiple stimuli. By combination of pattern and shape evolution, the coupled encryption of shape and pattern can be achieved. This approach empowers polymers with the ability to evolve under constant stimulus, offering insights into the functional design of polymer materials.

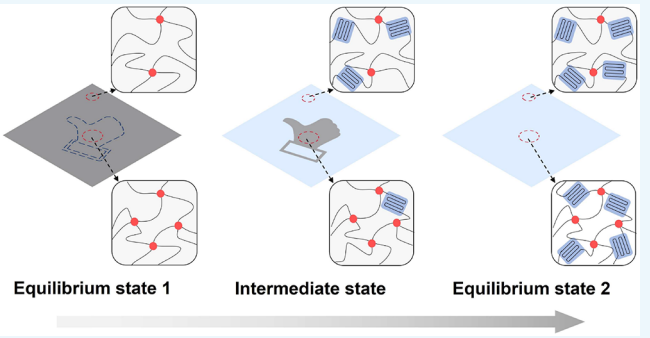

KEYWORDS: *evolution, programmability, crystallization-melting, information encryption, morphing materials*

INTRODUCTION

In the natural world, many creatures have evolved the ability to respond to the surrounding environment for survival.[1,2] For example, the octopus can alter its body shape and surface pattern to mimic various environments and other creatures. As inspired by biological systems, many intelligent polymer materials that can sense and respond to the external environment have been developed. These smart materials have shown promising applications in many fields including biomedicine,[3,4] information encryption,[5−7] and soft robotics.[8] At present, most stimuli-responsive materials can only exhibit a monotonic response to a single constant external stimulus, and the response pathway represents a naturally changing process (for instance, from one shape to another),[9] just like the leaves of mimosa change from opening to closing under stimulus (Figure 1a). However, in reality, the mimosa will adapt to the continuous harmless stimulus and open its leaves to obtain more sunlight.[10] This is similar to a non-monotonic change from opening to closing and again to opening under constant stimulus. Specifically, the initial and final states can be defined as equilibrium state 1 (ES1) and equilibrium state 2 (ES2), respectively; while the state in between is referred to as the intermediate state (IS). Achieving this transition between multiple states often requires the introduction of several different stimuli,[11−13] which may be challenging in some special environments such as in the human body or outer space. Therefore, it is significant to achieve non-monotonic evolution under constant external stimulus.

Programming the heterogeneous structure is an important way to design intelligent polymer materials. Common examples of heterogeneous structure include double-layer,[14] gradient,[15−17] and patterned structures.[17,18] The responsiveness of such materials can be achieved through the difference in the state of the heterogeneous structure when subjected to an external stimulus. Furthermore, it is worth noting that the non-monotonic change of materials can be realized by leveraging the differential evolution kinetics of structures in different regions. For example, the far-from-equilibrium shape-shifting of hydrogels was realized by varying the swelling kinetics in distinct regions,[9] and the multidirectional shape morphing was achieved by leveraging the rate discrepancy in the solvent desorption process across two sides of the material.[19] Nevertheless, due to the lack of evolution methods other than swelling or deswelling, such kind of non-monotonic

Received: March 14, 2024
Revised: May 14, 2024
Accepted: May 16, 2024
Published: May 24, 2024

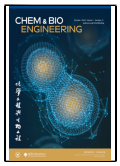

https://doi.org/10.1021/cbe.4c00058
Chem Bio Eng. 2024, 1, 790−797

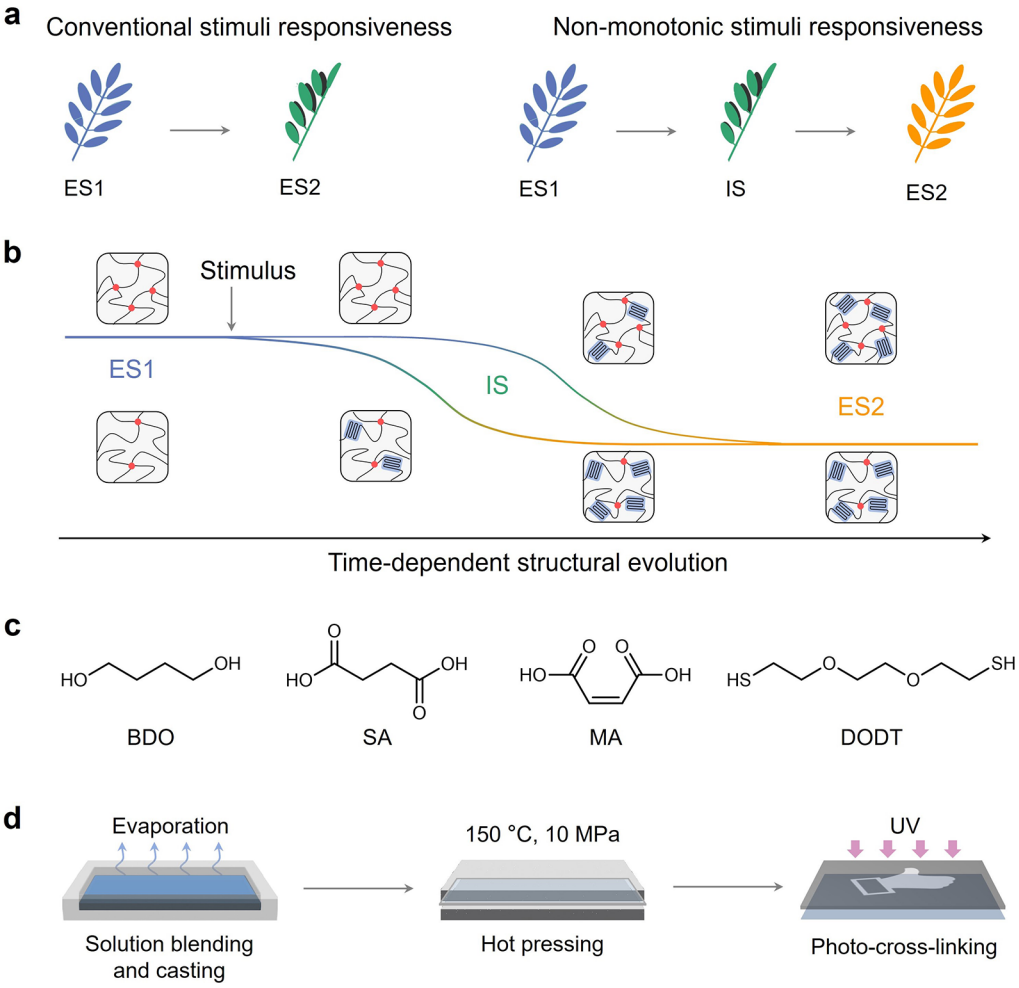

Figure 1. Design principle of the non-monotonic evolution material. (a) Schematic comparison between conventional and non-monotonic stimuli responsiveness. (b) Differential evolution dynamics of structures in more and less cross-linked regions to achieve non-monotonic stimuli responsiveness. (c) Chemical structure of monomer precursors and cross-linker of the non-monotonic evolution material. (d) Preparation of the polymer film and regulation of the cross-linking density by photo-cross-linking.

changes are only achieved in the solvent-containing material systems, and are still a challenge to be realized in dry materials.

Crystallization-melting is the most common phase transition of polymers, with over 70% of polymers being crystallizable. There are significant property differences for polymer materials between the crystalline and melting (or amorphous) states such as transparency, strength, modulus, and so on. By leveraging the crystallization-induced property differences, various functions such as pattern display[20] and shape morphing[21] can be realized in polymers. In addition, since the crystallization and melting processes are reversible, the phase structure and physical properties of the materials can be switched repeatedly by controlling the crystallization and melting. It is worth mentioning that the kinetics of crystallization-melting phase transition can be regulated by many factors such as molecular weight[22] and cross-linking degree (ρ_c).[23] By leveraging the spatial difference in the crystallization or melting kinetics of the materials, controllable evolution of properties and functions could be achieved. Therefore, the crystallization-melting phase transition holds the potential to serve as an evolution mechanism for achieving non-monotonic changes of dry materials.

Herein, we report a programming method to realize the non-monotonic evolution of pattern and shape in dry materials by spatially regulating the ρ_c in polymers to acquire spatial heterogeneous dynamics in the process of crystallization and melting. To achieve this idea, a polyester, poly(butylene succinate-*co*-butylene maleate) (PBSM), with double bond cross-linking sites on the main chain was synthesized as the model polymer matrix. The ρ_c of PBSM was manipulated by adjusting the irradiation time under ultraviolet (UV) light, and the spatial control of ρ_c was achieved through a photomask. Because ρ_c has a significant effect on the crystallization-melting kinetics, the remarkable differences in crystallization and melting kinetics between the regions possessing distinct ρ_c can be realized (Figure 1b), further leading to the spatial differences in transparency or shape recovery of the materials at a macroscopic scale. Upon completion of the crystallization or melting phase transformation, the physical properties (*e.g.*, transparency, shape recovery) of different regions tend to converge so as to realize the dynamic evolution of pattern information or shape. This design principle endows semi-crystalline polymer materials with the ability to evolve dynamically under a single constant stimulus, which can realize the application of multilevel information encryption and non-monotonic shape shifting. It is believed that this work could contribute novel insights into the design of functional polymer materials.

https://doi.org/10.1021/cbe.4c00058
Chem Bio Eng. 2024, 1, 790−797

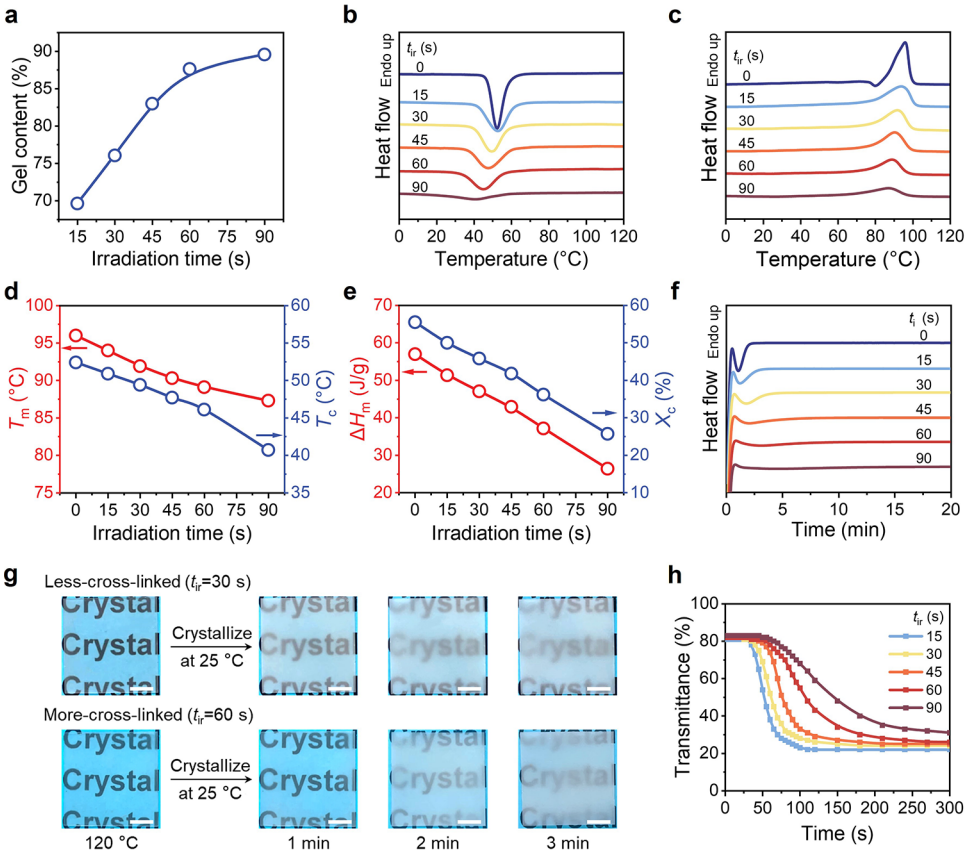

Figure 2. Characterization of the photo-cross-linked polymer films. (a) Gel content, (b) DSC curves collected upon cooling from 150 to −60 °C at 10 °C/min, (c) DSC curves collected upon heating from −60 to 150 °C at 10 °C/min, (d) Melting temperature (T_m) and crystallization temperature (T_c), (e) Melting enthalpy (ΔH_m) and crystallinity (X_c), and (f) Isothermal crystallization curves of the polymers with different irradiation times (t_{ir}). The samples were exposed under UV light for 15, 30, 45, 60, and 90 s, respectively. (g) Photos of the films (thickness ∼0.5 mm) with t_{ir} values of 30 and 60 s during crystallization. The samples were first melted at 120 °C and then placed at 25 °C. (h) Evolution of visible light transmittance upon cooling the films from 120 to 25 °C and holding at 25 °C for different time. All scale bars are 5 mm.

RESULTS AND DISCUSSION

To prepare the polymer network, we first synthesized unsaturated copolyester PBSM (M_w = 10.2 kDa) by melt polycondensation of 1,4-butanediol (BDO), succinic acid (SA), and maleic acid (MA) (Figure 1c). The synthesis process of PBSM is presented in Figure S1, and its chemical structural characterization can be found in Figure S2. Then, the copolyester was mixed with a sulfhydryl photo-cross-linking agent 3,6-dioxa-1,8-octanedithiol (DODT) and a photo-initiator 1-hydroxy cyclohexyl phenyl ketone (Irgacure-184) via solution blending. After removing the solvent by solution casting, the mixture was hot-pressed into a film (thickness ∼0.5 mm) and then photo-cross-linked under ultraviolet (UV) light for different durations (Figure 1d).

Fourier transform infrared (FTIR) spectroscopy of the film before and after UV irradiation was measured to prove the success of photo-cross-linking. The reduction of characteristic peaks (C═C stretch at 1642 cm^{-1}, ═C−H stretch at 3052 cm^{-1}, and S−H stretch at 2570 cm^{-1}) suggests a click reaction between the sulfhydryl group and double bond under UV light,[16,24] indicating successful cross-linking (Figure S3). The gel contents of polymer films with different UV irradiation times (t_{ir}) were measured by the solvent extraction method to explore the impact of t_{ir} on cross-linking. Figure 2a shows that the gel content increased from 70% to 90% with the extension of t_{ir} from 15 to 90 s, indicating an improvement in ρ_c. In addition, by measuring the apparent cross-linking density as a measure of ρ_c (Figure S4),[25,26] it is found that the cross-linking density increases with the increase of t_{ir}, which is consistent with the change of gel content.

Differential scanning calorimetry (DSC) measurements were conducted to evaluate the thermal behavior of cross-linked polyesters (Figure 2b, c). It can be seen that both the melting and crystallization temperatures (T_m, T_c) decrease gradually with the increase of t_{ir} (Figure 2d), due to the enhanced ρ_c. The crystallinity (X_c) of films with different t_{ir} was calculated by comparing the measured melting enthalpy (ΔH_m) with the standard melting enthalpy (ΔH_m^0), $X_c = \Delta H_m/\Delta H_m^0$, where ΔH_m was measured by DSC (Figure 2e) and ΔH_m^0 was obtained using the group contribution method (103 J/g for PBSM crystals).[27] Figure 2e shows that X_c decreases with increasing t_{ir}. Additionally, the DSC curves measured in isothermal crystallization also demonstrate a decrease in the crystallization rate as ρ_c increases (Figure 2f). Crystallization kinetic parameters of the polymers with different t_{ir} were calculated by the Avrami equation (Table S1). The crystallization time increases as ρ_c increases. Based on all the results discussed above, it is evident that the crystallization ability of a polymer film can be tuned by t_{ir}, due to the well-controlled ρ_c.

The mechanical stability of polymer film is crucial for their application.[28] We measured the mechanical property of the samples with different t_{ir} values (Figure S5a). The results show

https://doi.org/10.1021/cbe.4c00058
Chem Bio Eng. 2024, 1, 790−797

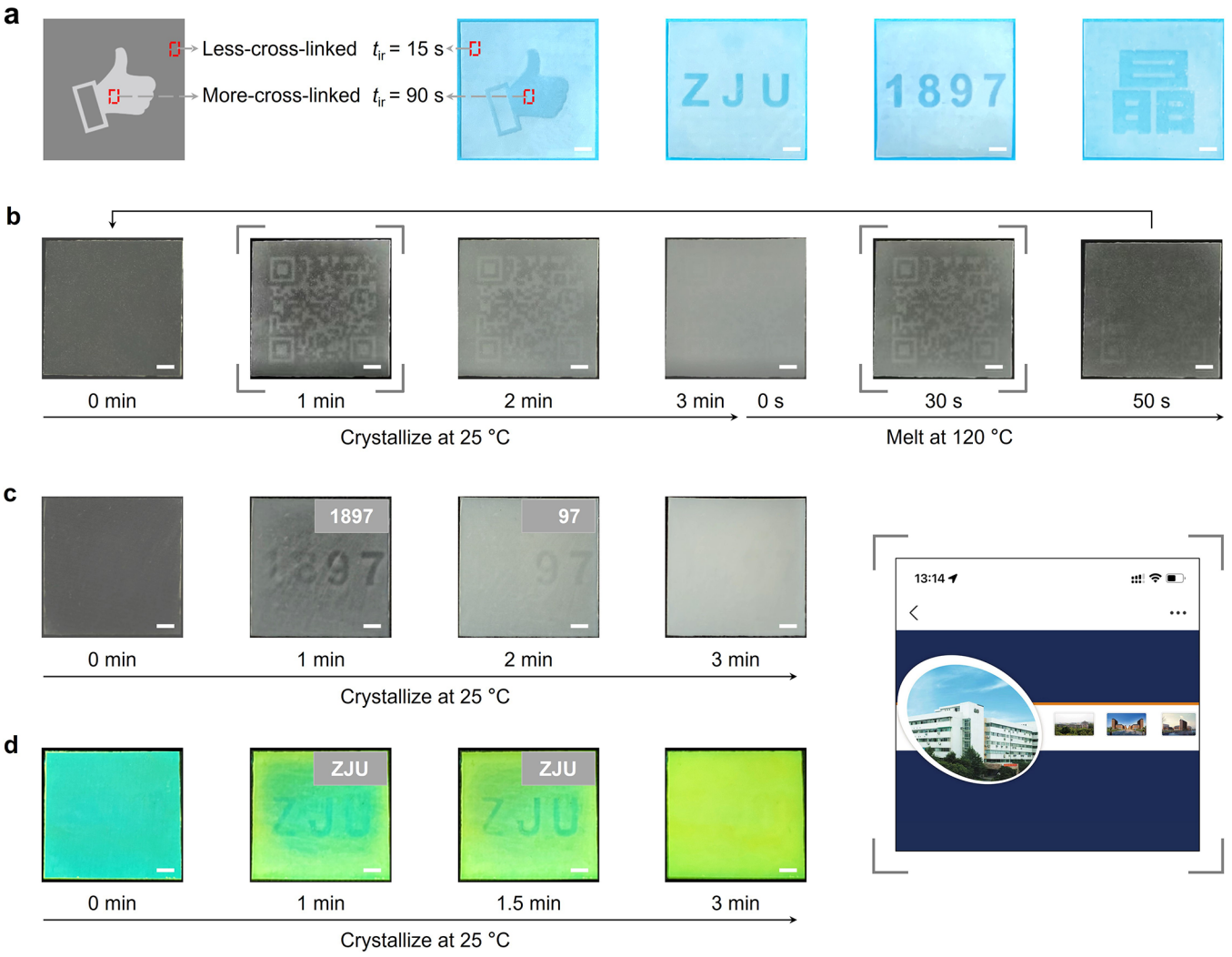

Figure 3. Evolution of pattern information. (a) Schematic illustration of patterned photo-cross-linking and information writing by patterned photo-cross-linking. The samples had two regions with t_{ir} values of 15 and 90 s. (b) Evolution of QR code pattern during crystallization at 25 °C and melting at 120 °C. The sample had two regions with t_{ir} values of 30 and 60 s. (c) Multistep dynamic evolution of pattern. The sample had three regions with t_{ir} values of 30, 45, and 60 s. (d) Evolution of the fluorescence pattern. The sample had two regions with t_{ir} values of 30 and 60 s, and fluorescent dye was added into the sample. All scale bars are 5 mm.

that with the extension of irradiation time, the tensile strength of the material decreases slightly and the elongation at break increases, which may be due to the decrease of X_c of the samples. For semicrystalline polymers, temperature will affect the crystallization-melt states and thus significantly affect their mechanical property. Therefore, taking the sample with t_{ir} of 45 s as an example, we measure its mechanical property at 25 °C (crystallization state) and at 120 °C (melting state) (Figure S5b). The results show that the polymer changes from hard to soft after melting, the tensile strength decreases significantly, and the elongation at break increases significantly.

Due to the effects of ρ_c on crystallization kinetics, the polymer films with different ρ_c show distinct transparency evolution in the cooling-induced crystallization process. In this experiment, the films with t_{ir} values of 30 and 60 s were first melted at 120 °C and then placed at 25 °C to observe the change of transparency (Figure 2g). The more-cross-linked film shows a slower decrease in transparency during crystallization, due to the slowed crystallization rate. As the crystallization proceeds, the two films eventually reach similar transparency. Also, the more-cross-linked film shows faster melting during heating (Figure S6). To quantify the transparency, we further used a transmission meter to measure the change of visible-light transmittance during crystallization for the films with various t_{ir} values (Figure 2h). It can be seen that, as the cross-linking time is prolonged, the transmittance of the films decreases more slowly due to the reduced crystallization rate. Except for the film whose crystallization ability is too weak after irradiation for 90 s, the transmittance of other films is similar after crystallization for 5 min.

We then spatially programmed the crystallization ability of the polymer film by locally tailoring the ρ_c with t_{ir}, as illustrated in Figure 3a. In the photo-cross-linking experiment, various regions within the film were exposed to UV light for different durations using a photomask, causing that the different regions have varied but well-controlled ρ_c, depicted as less-cross-linked and more-cross-linked regions. The more-cross-linked region with longer t_{ir} crystallizes more slowly during the cooling process than the less-cross-linked region with shorter t_{ir}. This different crystallization kinetics leads to variations in optical transparency between the two regions; thus, the crystal pattern can be displayed. By leveraging the pronounced difference in

https://doi.org/10.1021/cbe.4c00058
Chem Bio Eng. 2024, 1, 790−797

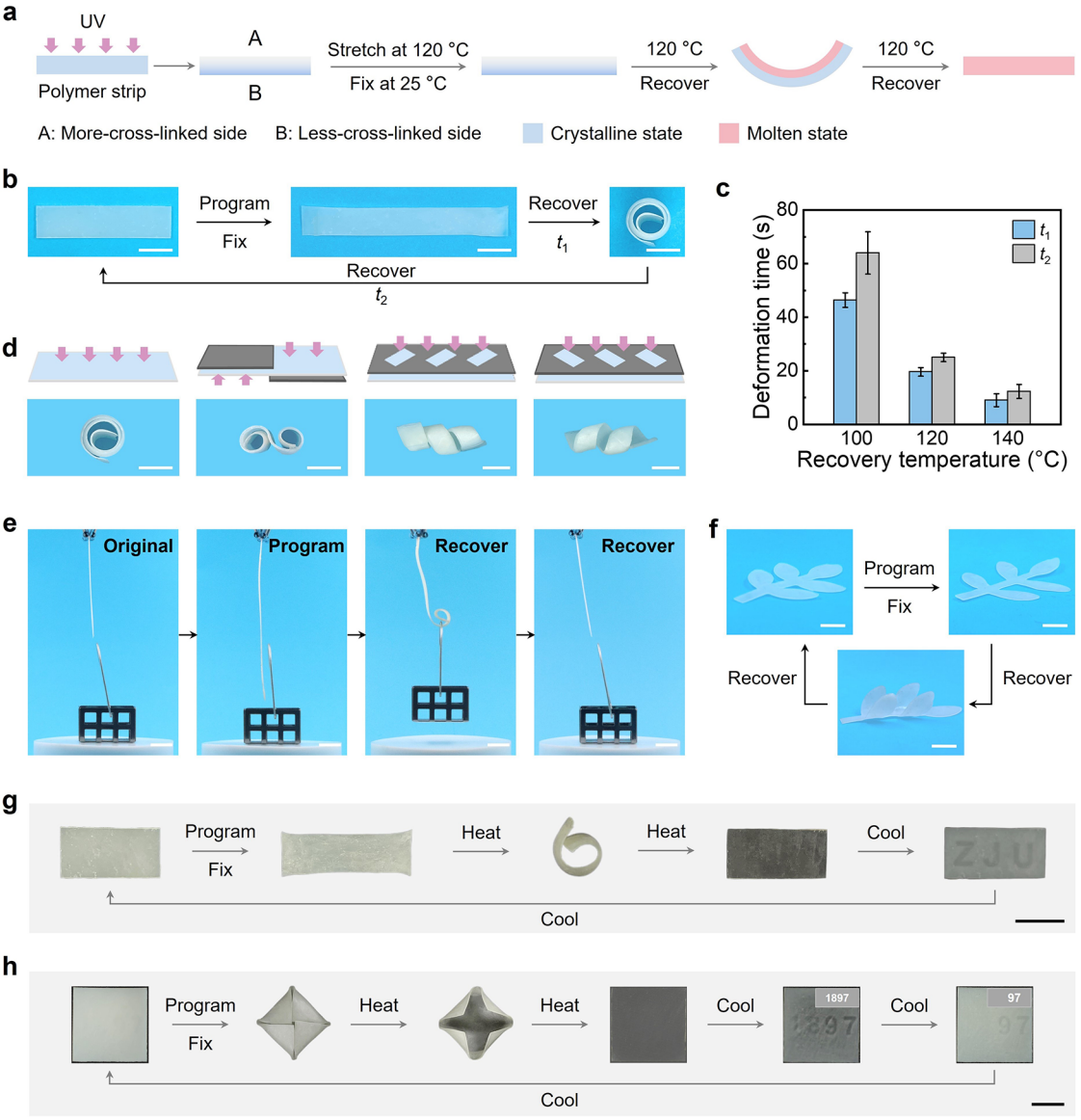

Figure 4. Non-monotonic shape evolution. (a) Schematic illustration of gradient photo-cross-linking and its resulting non-monotonic shape evolution. (b) Shape evolution of a gradient photo-cross-linked polymer film during the shape memory recovery process. (c) Non-monotonic shape evolution time at different recovery temperatures. t_1 is the evolution time from a flat shape to a curled shape in panel (b), and t_2 is the evolution time from a curled shape to a flat shape in panel (b). (d) Different shape evolution pathways based on patterned gradient photo-cross-linking. These shapes are the intermediate states of shape evolution. (e) Non-monotonic shape evolution for taking and releasing the objects. (f) Non-monotonic shape evolution to simulate the closing and reopening of mimosa. (g) Encryption/decryption process of a non-monotonic shape evolution film with pattern information. The encrypted information is "ZJU". (h) Encryption/decryption process of a multistep information evolution film folded into an envelope by origami method. "1897" is the interference information, and "97" is the encrypted information. All scale bars are 10 mm.

transparency during the crystallization process between the regions with t_{ir} of 15 and 90 s, we successfully achieved the display of crystal patterns, which could present diverse information such as graphics, letters, numbers, and Chinese characters (Figure 3a). The spatial resolution of these patterns was up to 100 μm (Figure S7).

Except for the writing of simple information, complex QR code information can be encrypted during the crystallization process (Figure 3b and Movie S1). To this end, a film was prepared with two regions exposed to irradiation for 30 and 60 s by using a photomask. The film was initially heated to 120 °C and completely melted and then allowed to crystallize at 25 °C. With the crystallization proceeding, the transparency difference between the two regions gradually increased, making the QR code visible and scannable with a smartphone to obtain the encoded information. With the completion of crystallization, all regions became opaque and the transparency difference decreased, causing the QR code information to gradually fade away after long-time crystallization. After the information disappeared, the film was heated to 120 °C for melting. Because the more-cross-linked region has lower T_m and X_c than the less-cross-linked region, the former melted faster than the latter during heating. Taking advantage of the different melting rates in the various regions during heating, we could also realize the appearance and evolution of the QR code. Furthermore, we expanded the approach by incorporating

https://doi.org/10.1021/cbe.4c00058
Chem Bio Eng. 2024, 1, 790−797

three regions with different t_{ir} (30, 45, and 60 s) to enable a multistep encryption of information. During the cooling process, the numbers "1897" and "97" could be read consecutively. Eventually, the information vanished as crystallization was completed (Figure 3c and Movie S2).

Moreover, it is worth noting that the crystallization of polymer chains can regulate the dispersion of doped fluorescent dyes in the polymer matrix, leading to a change in fluorescence color.[29] We then introduced the fluorescent dye 7-(diethylamino)coumarin-3-carboxylic acid and controlled the crystallization rates of different regions with t_{ir} values of 30 and 60 s. Accordingly, we are able to transform the evolution of crystal patterns into fluorescent patterns, which enrich the color of pattern evolution (Figure 3d and Movie S3). Our strategy serves as an effective means of information encryption and can be extended to other semicrystalline polymers. By selecting polymers with appropriate crystallization rates and incorporating more structural patterns, we believe that a wide range of editing possibilities of information evolution can be achieved. This encryption method hides the information in a specific process, and the decryption mechanism depends on the kinetics differences of the structural evolution of different regions. Thus, the information shows the dynamic nature of multistep change, which can improve the security of information to a great extent.

After studying the crystallization kinetics control in planar direction, we further investigated the crystallization control in the thickness direction by gradient cross-linking. Gradient structure is a common heterogeneous structure of polymer materials, which can be realized by the attenuation of light[16,30−32] or the diffusion of matter.[15,33] Figure 4a illustrates the strategy to induce the gradient cross-linking structure in polymer film. In this experiment, the solution-cast film comprising of PBSM, photo-cross-linker, and photoinitiator was exposed to UV light on one side for 30 s to establish a gradient in ρ_c, utilizing the attenuation of light intensity along the thickness direction. The gradient structure of the as-prepared film was confirmed by wide-angle X-ray scattering (WAXS) and DSC (Figure S8). The WAXS results show that the diffraction intensity of the side near the UV light was lower than that far from the UV light, due to the higher ρ_c of the side near the UV light. The DSC results collected in the heating and cooling process are consistent with the WAXS results. The gradient structure of cross-linked polymer film was also verified by scanning electron microscopy (SEM) (Figure S9). Before SEM measurement, the sample was immersed in chloroform to etch the non-cross-linked part. It can be seen that the non-cross-linked part etched away is less in the top side, indicating the higher ρ_c. On the contrary, the bottom side shows more etching parts due to the lower ρ_c. Therefore, ρ_c decreased with the attenuation of light intensity. As deduced from former results (Figure 1d, e), T_m, and X_c will vary gradiently and there will be multistep melting behavior along the thickness direction.

According to the shape morphing mechanism of shape memory polymers triggered by melt-crystallization transition,[34−36] the shape shifting can be triggered by the melting of crystals. Based on this principle, we hypothesize that the multistep melting behavior can be employed to program the non-monotonic shape evolution during the shape recovery process. The shape memory properties of gradiently cross-linked film were measured using a dynamic mechanical analyzer (DMA). The film demonstrated the shape fixity rate (R_f) and shape recovery rate (R_r) exceeding 99% and 96%, respectively, over four shape memory cycles (Figure S10). To validate the aforementioned non-monotonic shape evolution hypothesis, the film was stretched by 50% at 120 °C, then cooled to 25 °C to fix its temporary shape, and then heated to the elevated temperature to observe the shape recovery behavior (Figure 4b and Movie S4). The result shows that the film first curled and then unfolded during the shape recovery process, displaying a non-monotonic shape evolution consistent with our prediction. This behavior arises from the presence of a gradient crystal structure, which leads to different melting kinetics in the film thickness direction. Shape recovery starts on the more-cross-linked side and then progresses to the opposite less-cross-linked side, resulting in the non-monotonic shape evolution (Figure 4a). For comparing the shape morphing behavior between gradiently cross-linked and uniformly cross-linked films, we prepared a uniformly cross-linked film by irradiating both sides with UV light for 15 s and explored its shape memory effect (Figure S11). The result shown that, compared to the gradiently cross-linked film, the uniformly cross-linked film only exhibited the monotonous shrinkage but not the controllable multistep deformation. Additionally, the shape evolution time from the temporary shape to the curled shape (t_1) and from the curled shape to the permanent shape (t_2) were measured during the shape recovery process at different recovery temperatures (Figure 4c and Figure S12). It was found that the shape morphing became faster with the recovery temperature rising and the non-monotonic shape evolution always took place at even elevated temperatures.

Combined with the local control over strain,[37] complex and diverse shape evolution can be realized during the shape recovery process (Figure 4d). The non-monotonic shape evolution of the film can be utilized to pick up the object when curling and then put the object down when unfolding (Figure 4e and Movie S5). This controllable non-monotonic shape evolution under a single constant stimulus is difficult to attain using other programming methods. Furthermore, we cut the film into the shape of a starfish. It was stretched in the molten state (120 °C) and then crystallized to fix the temporary shape. Afterwards, upon thermal stimulus (heating to 120 °C), the starfish flexed its body to pass through the narrow hole and then opened its body (Figure S13 and Movie S6). According to this programming principle, diversified and process-controllable shape evolution design can be realized by cutting the film into various shapes and combined with the means of patterned irradiation, for example, the non-monotonic shape evolution of mimosa and flower (Figure 4f and Figure S14). This strategy enables the material to undergo dynamic shape changes under a constant stimulus, thereby enhancing its potential for functional application.

Furthermore, multiple encryptions of information can be realized by coupling the pattern and shape evolution of the material. As shown in Figure 4g, we encrypted a film with "ZJU" information (like Figure 2b, the sample had two regions with t_{ir} of 30 and 60 s) into a stretched temporary shape. During the decryption process, the film initially curled upon heating, thus, concealing the information inside. As the film is unfolded in the end of shape recovery process, the information became readable with the first crystallization of less-cross-linked region and it was hidden again with the subsequent crystallization of more-cross-linked region. In addition, we encrypted the pattern information capable of multistage

https://doi.org/10.1021/cbe.4c00058
Chem Bio Eng. 2024, 1, 790−797

evolution in the film (like Figure 2c, the sample had three regions with t_{ir} of 30, 45, and 60 s) and then programmed it into a shape similar to an envelope by the shape memory mechanism and origami method (Figure 4h). To access the information inside, it was needed to open the envelope by heating first (Movie S7), and then the number information could be read during the cooling process. During the evolution of pattern information, "1897" can be set as the interference information and "97" as the real information. Eventually, the information vanished as crystallization was completed.

CONCLUSION

In summary, we propose a novel method to achieve pattern and shape evolution in dry materials by a spatially programmed crystallization and melting process. The design principle is using light to regulate the spatial cross-linking structure of the polymer, thus endowing the material with spatially distinct crystallization and melting kinetics to realize the controllable property evolution over time. First, pattern evolution offers an ingenious approach to hide the information in a specific process, and the dynamic nature of multistep change improves the information security to a great extent. Second, shape evolution enables the material with non-monotonic shape morphing ability, which can achieve controllable shape switching under a single constant stimulus, simplifying the external conditions to achieve complex shape morphing. Furthermore, the combination of pattern and shape evolution provides a more secure encryption method that couples the dual encryption of pattern and shape. We believe that this programming approach can offer new insights into the functional design of polymer materials.

ASSOCIATED CONTENT

Supporting Information

The Supporting Information is available free of charge at https://pubs.acs.org/doi/10.1021/cbe.4c00058.

Materials, methods, synthesis, ^{1}H NMR spectrum, FTIR spectra, apparent cross-linking density, isothermal crystallization kinetic parameters, mechanical properties, photos of the films during the melting process, spatial resolution of photo-patterning, WAXS profiles, DSC curves, SEM image, shape memory performances, monotonic shape-shifting of the uniformly cross-linked film, and non-monotonic shape evolution of the gradiently cross-linked films (PDF)

Time evolution of QR code (MP4)

Multistep dynamic evolution of the information patterns (MP4)

Time evolution of the fluorescent pattern (MP4)

Non-monotonic shape evolution (MP4)

Non-monotonic shape evolution for taking and releasing the objects (MP4)

Non-monotonic shape evolution to pass through the narrow hole (MP4)

Opening process of a film folded into an envelope (MP4)

AUTHOR INFORMATION

Corresponding Authors

Pengju Pan − *State Key Laboratory of Chemical Engineering, College of Chemical and Biological Engineering, Zhejiang University, Hangzhou 310058, China; Institute of Zhejiang University-Quzhou, Quzhou 324000, China;* orcid.org/0000-0001-6924-5485; Email: panpengju@zju.edu.cn

Chengtao Yu − *State Key Laboratory of Chemical Engineering, College of Chemical and Biological Engineering, Zhejiang University, Hangzhou 310058, China; Institute of Zhejiang University-Quzhou, Quzhou 324000, China;* orcid.org/0000-0002-3656-0582; Email: yuchengtao@zju.edu.cn

Authors

Xing Zhang − *State Key Laboratory of Chemical Engineering, College of Chemical and Biological Engineering, Zhejiang University, Hangzhou 310058, China*

Yichen Zhou − *State Key Laboratory of Chemical Engineering, College of Chemical and Biological Engineering, Zhejiang University, Hangzhou 310058, China*

Mengzhe Han − *State Key Laboratory of Chemical Engineering, College of Chemical and Biological Engineering, Zhejiang University, Hangzhou 310058, China*

Ying Zheng − *State Key Laboratory of Chemical Engineering, College of Chemical and Biological Engineering, Zhejiang University, Hangzhou 310058, China; Institute of Zhejiang University-Quzhou, Quzhou 324000, China;* orcid.org/0000-0002-2379-6342

Junfeng Liu − *State Key Laboratory of Chemical Engineering, College of Chemical and Biological Engineering, Zhejiang University, Hangzhou 310058, China; Institute of Zhejiang University-Quzhou, Quzhou 324000, China*

Yongzhong Bao − *State Key Laboratory of Chemical Engineering, College of Chemical and Biological Engineering, Zhejiang University, Hangzhou 310058, China; Institute of Zhejiang University-Quzhou, Quzhou 324000, China*

Guorong Shan − *State Key Laboratory of Chemical Engineering, College of Chemical and Biological Engineering, Zhejiang University, Hangzhou 310058, China; Institute of Zhejiang University-Quzhou, Quzhou 324000, China;* orcid.org/0000-0001-5676-6310

Complete contact information is available at: https://pubs.acs.org/10.1021/cbe.4c00058

Author Contributions

The manuscript was written through contributions of all authors. All authors have given approval to the final version of the manuscript.

Notes

The authors declare no competing financial interest.

ACKNOWLEDGMENTS

This research was financially supported by National Natural Science Foundation of China (U22A20400, 52103020), National Natural Science Foundation of Zhejiang Province (LHDMZ23E030001) and State Key Laboratory of Chemical Engineering (SKL-ChE-23T05).

REFERENCES

(1) Taboada, C.; Delia, J.; Chen, M.; Ma, C.; Peng, X.; Zhu, X.; Jiang, L.; Vu, T.; Zhou, Q.; Yao, J.; O'Connell, L.; Johnsen, S. Glassfrogs Conceal Blood in Their Liver to Maintain Transparency. *Science* **2022**, *378*, 1315−1320.

(2) Woo, T.; Liang, X.; Evans, D. A.; Fernandez, O.; Kretschmer, F.; Reiter, S.; Laurent, G. The Dynamics of Pattern Matching in Camouflaging Cuttlefish. *Nature* **2023**, *619*, 122−128.

(3) Lendlein, A.; Langer, R. Biodegradable, Elastic Shape-Memory Polymers for Potential Biomedical Applications. *Science* **2002**, *296*, 1673−1676.
(4) Zhao, W.; Yue, C.; Liu, L.; Liu, Y.; Leng, J. Research Progress of Shape Memory Polymer and 4D Printing in Biomedical Application. *Adv. Healthc. Mater.* **2023**, *12*, 2201975.
(5) Zhu, C. N.; Bai, T.; Wang, H.; Ling, J.; Huang, F.; Hong, W.; Zheng, Q.; Wu, Z. L. Dual-Encryption in a Shape-Memory Hydrogel with Tunable Fluorescence and Reconfigurable Architecture. *Adv. Mater.* **2021**, *33*, 2102023.
(6) Li, Z.; Zhang, C.; Huang, W.; Cui, C.; Chen, K.; He, Z.; Xu, T.; Teng, H.; Ge, Z.; Ming, X.; Zhang, Y. 3D-Printable Room Temperature Phosphorescence Polymer Materials with On-Demand Modulation for Modulus Visualization and Anticounterfeiting Applications. *Chem. Bio Eng.* **2024**, *1*, 133−140.
(7) Shang, H.; Le, X.; Sun, Y.; Shan, F.; Wu, S.; Zheng, Y.; Li, D.; Guo, D.; Liu, Q.; Chen, T. Integrating Photorewritable Fluorescent Information in Shape-Memory Organohydrogel Toward Dual Encryption. *Adv. Opt. Mater.* **2022**, *10*, 2200608.
(8) Zhao, Y.; Hua, M.; Yan, Y.; Wu, S.; Alsaid, Y.; He, X. Stimuli-Responsive Polymers for Soft Robotics. *Annu. Rev. Control Robot. Auton. Syst.* **2022**, *5*, 515−545.
(9) Zhang, Y.; Liu, K.; Liu, T.; Ni, C.; Chen, D.; Guo, J.; Liu, C.; Zhou, J.; Jia, Z.; Zhao, Q.; Pan, P.; Xie, T. Differential Diffusion Driven Far-From-Equilibrium Shape-Shifting of Hydrogels. *Nat. Commun.* **2021**, *12*, 6155.
(10) Gagliano, M.; Renton, M.; Depczynski, M.; Mancuso, S. Experience Teaches Plants to Learn Faster and Forget Slower in Environments Where It Matters. *Oecologia* **2014**, *175*, 63−72.
(11) Feng, Y.; Ma, Z.; Zhong, S.; Wang, C.; Chen, X. Stepwise Stimuli-Responsive, Multicolor-Chromic Perylene Bisimide/Polyvinyl Alcohol Co-assembly System for Information Encryption. *Chem.—Eur. J.* **2023**, *29*, No. e202301074.
(12) Wang, Y.; Zhu, Y.; Wang, J.; Li, X.; Wu, X.; Qin, Y.; Chen, W. Fe3+, NIR Light and Thermal Responsive Triple Network Composite Hydrogel with Multi-Shape Memory Effect. *Compos. Sci. Technol.* **2021**, *206*, No. 108653.
(13) Xiang, Y.; Liu, C.; Ma, S.; Wang, X.; Zhu, L.; Bao, C. Stimuli-Responsive Peptide Self-Assembly to Construct Hydrogels with Actuation and Shape Memory Behaviors. *Adv. Funct. Mater.* **2023**, *33*, 2300416.
(14) Chen, S.; Hu, J.; Zhuo, H.; Zhu, Y. Two-Way Shape Memory Effect in Polymer Laminates. *Mater. Lett.* **2008**, *62*, 4088−4090.
(15) Yang, L.; Zhang, G.; Zheng, N.; Zhao, Q.; Xie, T. A Metallosupramolecular Shape-Memory Polymer with Gradient Thermal Plasticity. *Angew. Chem. Int. Ed.* **2017**, *129*, 12773−12776.
(16) Yang, Q.; Shahsavan, H.; Deng, Z.; Guo, H.; Zhang, H.; Liu, H.; Zhang, C.; Priimagi, A.; Zhang, X.; Zeng, H. Semi-Crystalline Rubber as a Light-Responsive, Programmable. *Resilient Robotic Material. Adv. Funct. Mater.* **2022**, *32*, 2206939.
(17) Ding, M.; Yuan, W.; Xu, S.; Yu, C.; Zheng, Y.; Zhou, J.; Shan, G.; Bao, Y.; Pan, P. Light-Induced Crystalline Size Heterogeneity of Polymers Enables Programmable Writing, Morphing, and Mechanical Performance Designing. *ACS Macro Lett.* **2022**, *11*, 739−746.
(18) Huang, L.; Jiang, R.; Wu, J.; Song, J.; Bai, H.; Li, B.; Zhao, Q.; Xie, T. Ultrafast Digital Printing toward 4D Shape Changing Materials. *Adv. Mater.* **2017**, *29*, 1605390.
(19) Chen, W.; Zhang, X.; Yang, X.; Yang, B.; Chen, D.; Lei, Y.; Liu, S.; Xue, L. Bioinspired Anisotropic PEEK for Solvent Sensing and Programmable Actuations. *Chem. Eng. J.* **2023**, *468*, No. 143808.
(20) Qiu, Y.; Munna, D.; Wang, F.; Xi, J.; Wang, Z.; Wu, D. Regulating Asynchronous Deformations of Biopolyester Elastomers via Photoprogramming and Strain-Induced Crystallization. *Macromolecules* **2021**, *54*, 5694−5704.
(21) Zhuo, S.; Song, C.; Rong, Q.; Zhao, T.; Liu, M. Shape and Stiffness Memory Ionogels with Programmable Pressure-Resistance Response. *Nat. Commun.* **2022**, *13*, 1743.
(22) Safari, M.; Martínez De Ilarduya, A.; Mugica, A.; Zubitur, M.; Muñoz-Guerra, S.; Müller, A. J. Tuning the Thermal Properties and Morphology of Isodimorphic Poly[(butylene succinate)-ran-(ε-caprolactone)] Copolyesters by Changing Composition, Molecular Weight, and Thermal History. *Macromolecules* **2018**, *51*, 9589−9601.
(23) Deng, S.; Huang, L.; Wu, J.; Pan, P.; Zhao, Q.; Xie, T. Bioinspired Dual-Mode Temporal Communication via Digitally Programmable Phase-Change Materials. *Adv. Mater.* **2021**, *33*, 2008119.
(24) Liang, H.; Wu, Y.; Zhang, Y.; Chen, E.; Wei, Y.; Ji, Y. Elastomers Grow into Actuators. *Adv. Mater.* **2023**, *35*, 2209853.
(25) Rahman, M. A.; Sartore, L.; Bignotti, F.; Di Landro, L. Autonomic Self-Healing in Epoxidized Natural Rubber. *ACS Appl. Mater. Interfaces* **2013**, *5*, 1494−1502.
(26) Choi, S.; Han, D. Strain effect on recovery behaviors from circular deformation of natural rubber vulcanizate. *J. Appl. Polym. Sci.* **2009**, *114*, 935−939.
(27) Van Krevelen, D. W.; Te Nijenhuis, K. Calorimetric Properties. In *Properties of Polymers*, Fourth ed.; Elsevier: Amsterdam, 2009; Chapter 5, pp 109−128.
(28) He, Z.; Liu, Z.; Liu, B.; Wang, K.; Dong, X.; Zhang, Z.; Chen, C.; Wang, M.; Liu, J.; Huang, W. Thermally-induced phase fusion and color switching in ionogels for multilevel information encryption. *Chem. Eng. J.* **2024**, *479*, No. 147544.
(29) Du, J.; Sheng, L.; Chen, Q.; Xu, Y.; Li, W.; Wang, X.; Li, M.; Zhang, S. X. Simple and General Platform for Highly Adjustable Thermochromic Fluorescent Materials and Multi-Feasible Applications. *Mater. Horiz.* **2019**, *6*, 1654−1662.
(30) Wang, S.; Kaneko, D.; Okajima, M.; Yasaki, K.; Tateyama, S.; Kaneko, T. Hyperbranched Polycoumarates with Photofunctional Multiple Shape Memory. *Angew. Chem. Int. Ed.* **2013**, *52*, 11143−11148.
(31) Lu, Y.; Zhang, C.; Xie, T.; Wu, J. Grayscale Color 3D/4D Printing Via Orthogonal Photochemistry. *Chem. Bio Eng.* **2024**, *1*, 76−82.
(32) Yasaki, K.; Suzuki, T.; Yazawa, K.; Kaneko, D.; Kaneko, T. Effects of Double Photoreactions on Polycoumarate Photomechanics. *J. Polym. Sci., Part A: Polym. Chem.* **2011**, *49*, 1112−1118.
(33) Li, G.; Wang, S.; Liu, Z.; Liu, Z.; Xia, H.; Zhang, C.; Lu, X.; Jiang, J.; Zhao, Y. 2D-to-3D Shape Transformation of Room-Temperature-Programmable Shape-Memory Polymers through Selective Suppression of Strain Relaxation. *ACS Appl. Mater. Interfaces* **2018**, *10*, 40189−40197.
(34) Lendlein, A.; Gould, O. E. C. Reprogrammable Recovery and Actuation Behaviour of Shape-Memory Polymers. *Nat. Rev. Mater.* **2019**, *4*, 116−133.
(35) Zare, M.; Prabhakaran, M. P.; Parvin, N.; Ramakrishna, S. Thermally-Induced Two-Way Shape Memory Polymers: Mechanisms, Structures, and Applications. *Chem. Eng. J.* **2019**, *374*, 706−720.
(36) Zhao, Q.; Qi, H. J.; Xie, T. Recent Progress in Shape Memory Polymer: New Behavior, Enabling Materials, and Mechanistic Understanding. *Prog. Polym. Sci.* **2015**, *49*−*50*, 79−120.
(37) Yuan, W.; Xu, S.; Yu, C.; Ding, M.; Zheng, Y.; Zhou, J.; Shan, G.; Bao, Y.; Pan, P. Photothermal Driven Polymorph Pattern in Semicrystalline Polymers Towards Programmable Shape Morphing. *Chem. Eng. J.* **2022**, *446*, No. 137346.

https://doi.org/10.1021/cbe.4c00058
Chem Bio Eng. 2024, 1, 790−797